# Supporting Information

## Human Interactive Triboelectric Nanogenerator as a Self-Powered Smart Seat

Arunkumar Chandrasekhar[1], Nagamalleswara Rao Alluri[2], Balasubramaniam Saravanakumar[3], Sophia Selvarajan[4], Sang-Jae Kim [1*]

[1,3*] Nanomaterials and System Lab, Department of Mechatronics Engineering, Jeju National University, Jeju 690-756, Republic of Korea

[2] Faculty of Applied Energy System, Department of Mechanical Engineering, Jeju National University, Jeju 690-756, Republic of Korea

[4] Department of the Next Generation Convergence Technology, Jeju National University, Jeju 690-756, Republic of Korea

*Corresponding author: Tel: +82-64-754-3715; Fax: +82-64-756-3886

Email:kimsangj@jejunu.ac.kr (Prof. Sang-Jae Kim)

| No | Materials | Triboelectric charge | Role of Action |
|---|---|---|---|
| 1 | Aluminum | Positive | Electrode |
| 2 | Paper | Positive | Contact Material |
| 3 | Cotton | Positive | Contact Material |
| 4 | Polyethylene<br><br>(Polyethylene Cover) | Negative | Contact Material |
| 5 | Polyimide (Kapton) | Negative | Active layer |
| 6 | Poly Vinyl Chloride (Bus Card) | Negative | Contact Material |

**Table S1**. The triboelectric series: a list that ranks various materials used for the SS-TENG studies, according to their tendency to lose electrons (positive) or gain (negative) in frictional charging and contact charging process.

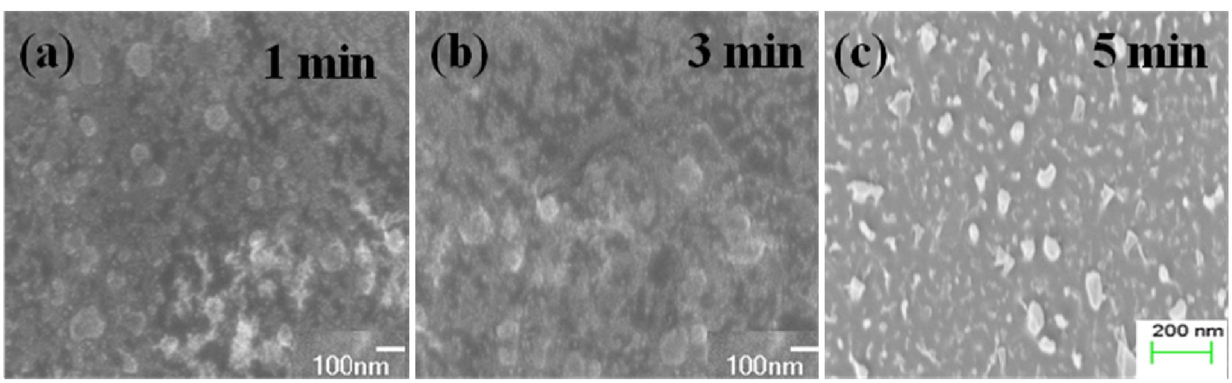


**Figure S1.** FE-SEM images of negatively charged triboelectric active layer: Plasma treated Kapton at different time period (a) 1 min, (b) 3 min and (c) 5 min.

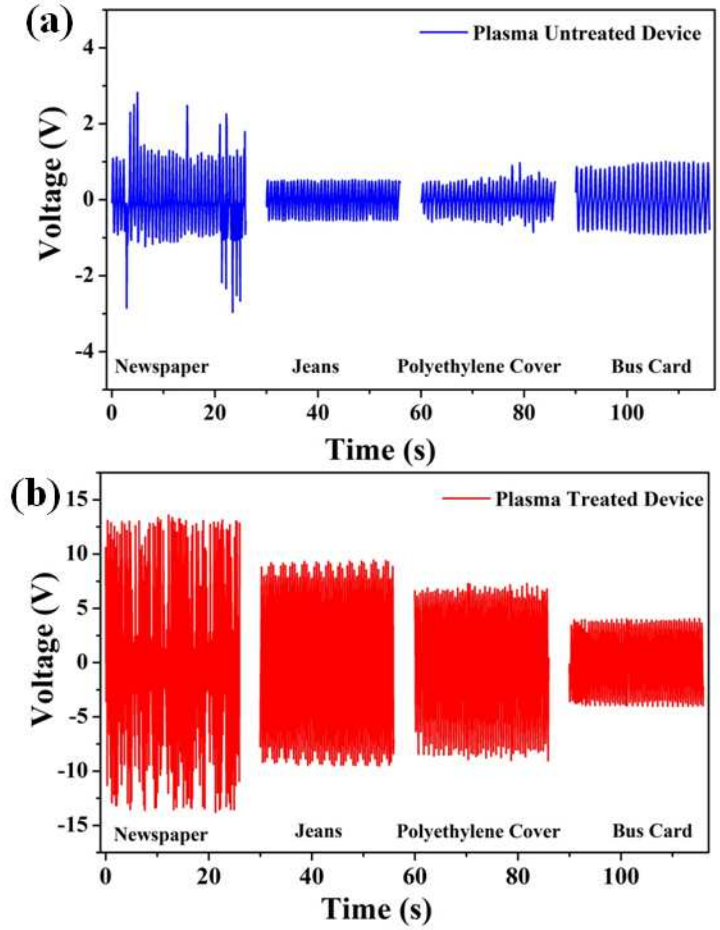


**Figure S2**. (a) Output voltage response of SS-TENG using Plasma Non treated Kapton film as the active layer. (b) Output voltage response of SS-TENG using Plasma treated Kapton film as the active layer.

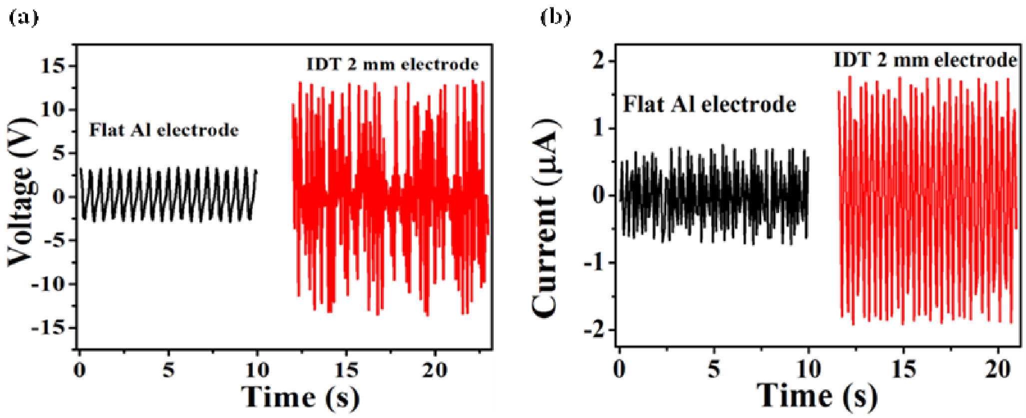


**Figure S3.** (a) Output voltage and (b) current response of SS-TENG using flat Al electrode and IDT 2 mm electrode.

Initially, we started SS-TENG concept in plain Al electrode, which showed poor performance to drive a low power electronic device. These results gave us another perspective to search in detail regarding the influence of structured electrode in single electrode mode TENG. Usually structured electrode enhances the charge transfer efficiency in sliding mode,[1,2] this motivated us to study in detail regarding structured electrodes for our SS-TENG. Recently few articles have been published with IDT electrode structure based TENG and successfully applied for the self-powered applications.[2,3] As IDT electrode are most commonly used in sliding mode (two electrodes) TENG.[3] We adopted this structure to study its performance as a single electrode in contact and separation mode TENG. So we fabricated an IDT electrode of minimum dimension (50 mm by 2 mm, separated by a gap of 2 mm) feasible by our laser cutting instrument. This rapid enlargement in the electrical signal forced to find the hidden mechanism called **Edge effect.**[4–6] It was observed that the interaction with charged surface and the value of current was very high at the corners compared to other plain electrode due to the edge effect.[7,8] Hence, we further carried our research to study the device performance fabricated using IDT electrode.

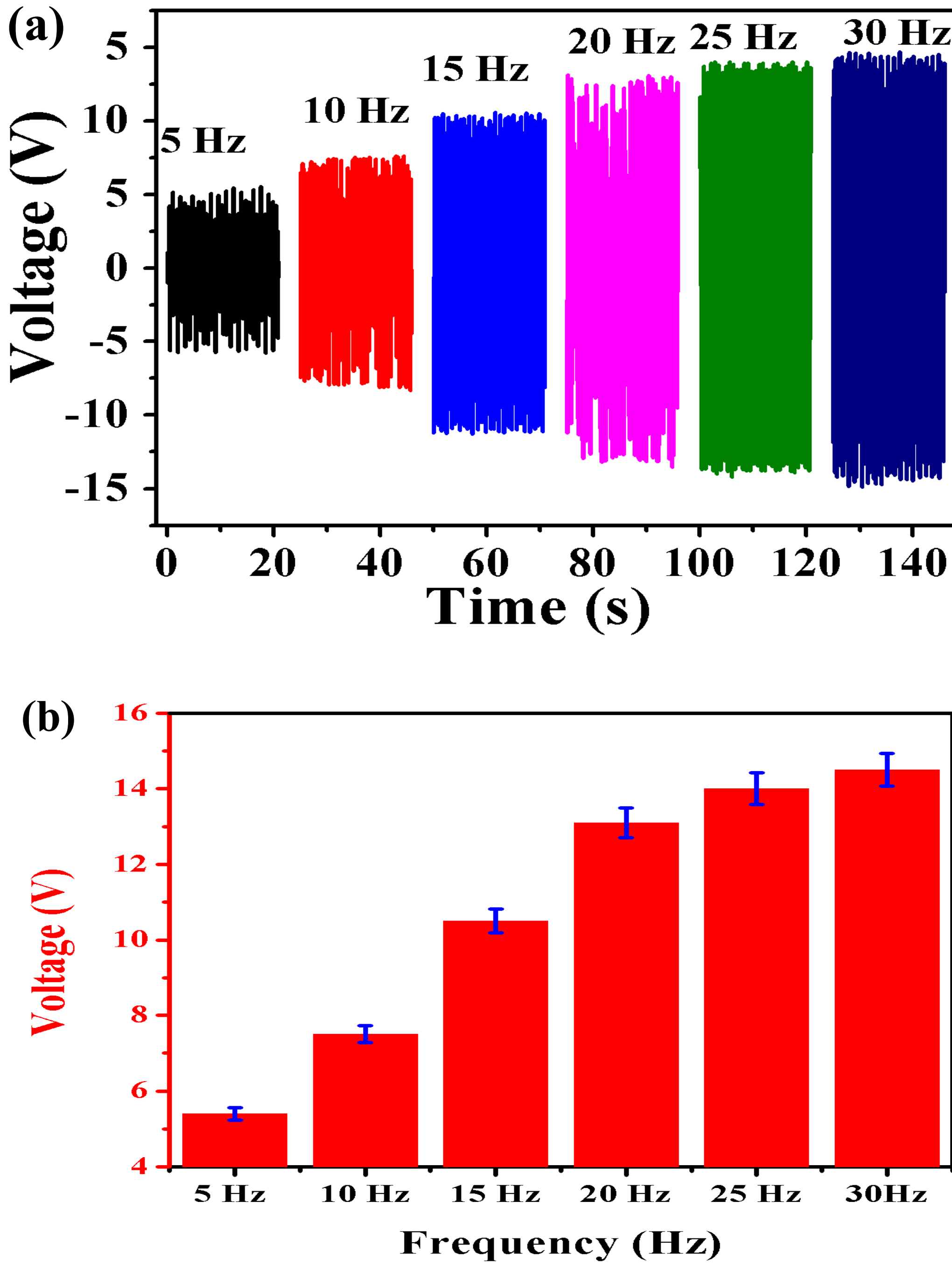


**Figure S4.** (a) The measured output voltage at different cyclic frequency of 5Hz, 10Hz, 15 Hz, 20 Hz, 25Hz, and 30Hz and (b) error limits of measured output voltage at different cyclic frequency.

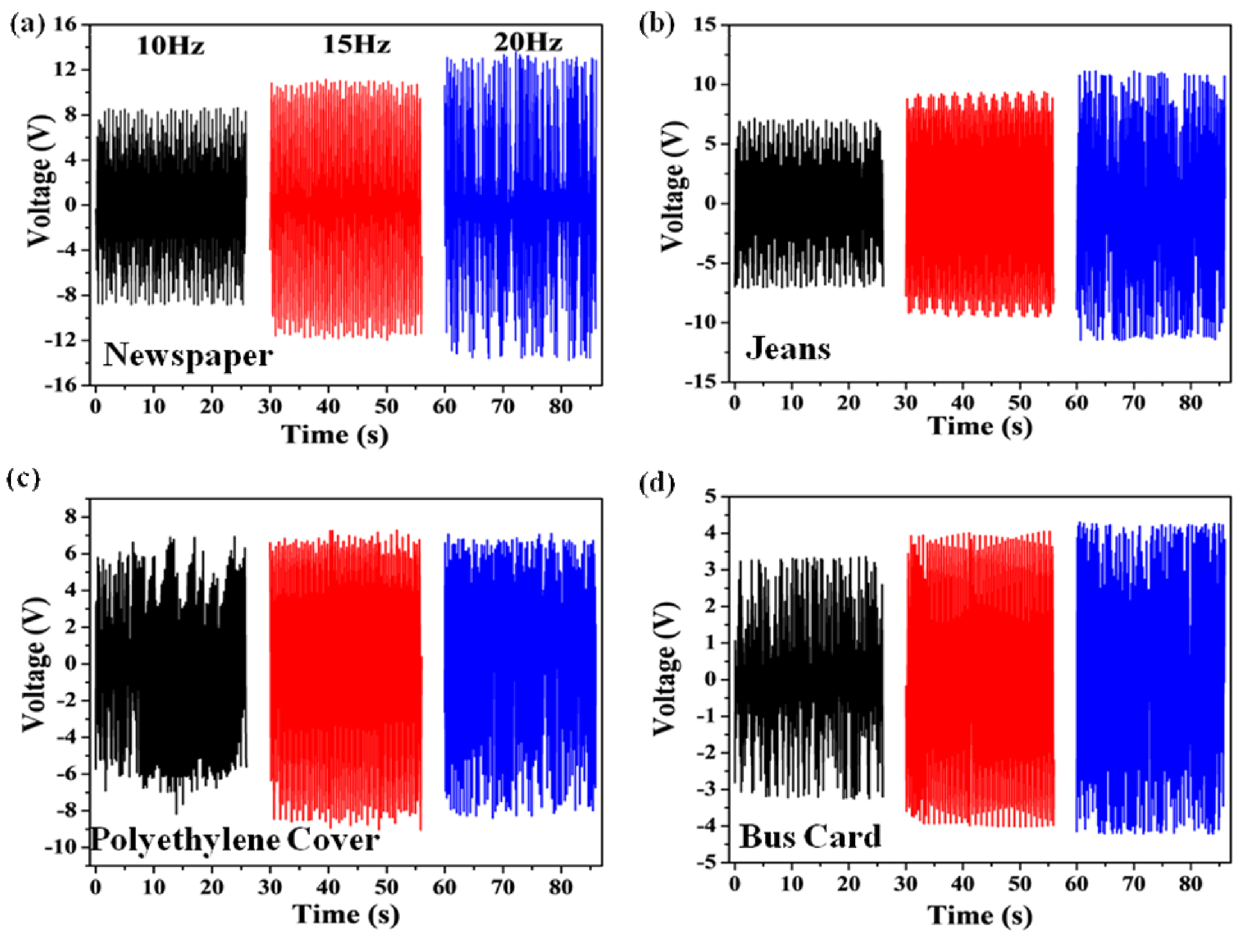


**Figure S5**. The measured output voltage of four materials with SS-TENGs at different cyclic frequency of 10, 15 and 20 Hz. (a-d) When the SS-TENG has interaction with Newspaper, Jeans cloth, Polyethylene cover and Bus card respectively.

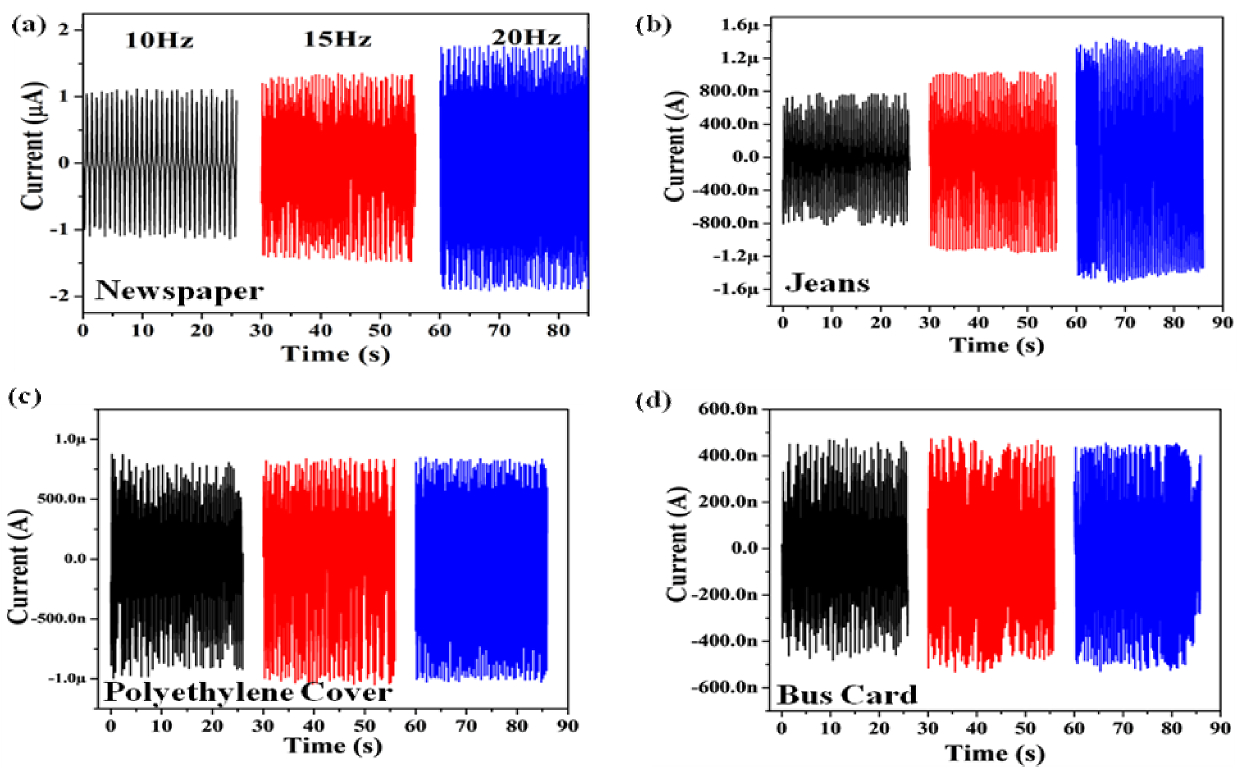


**Figure S6**. The measured output current of four materials with SS-TENGs at different cyclic frequency of 10, 15 and 20 Hz. (a-d) When the SS-TENG has interaction with Newspaper, Jeans cloth, Polyethylene cover, Bus card respectively.

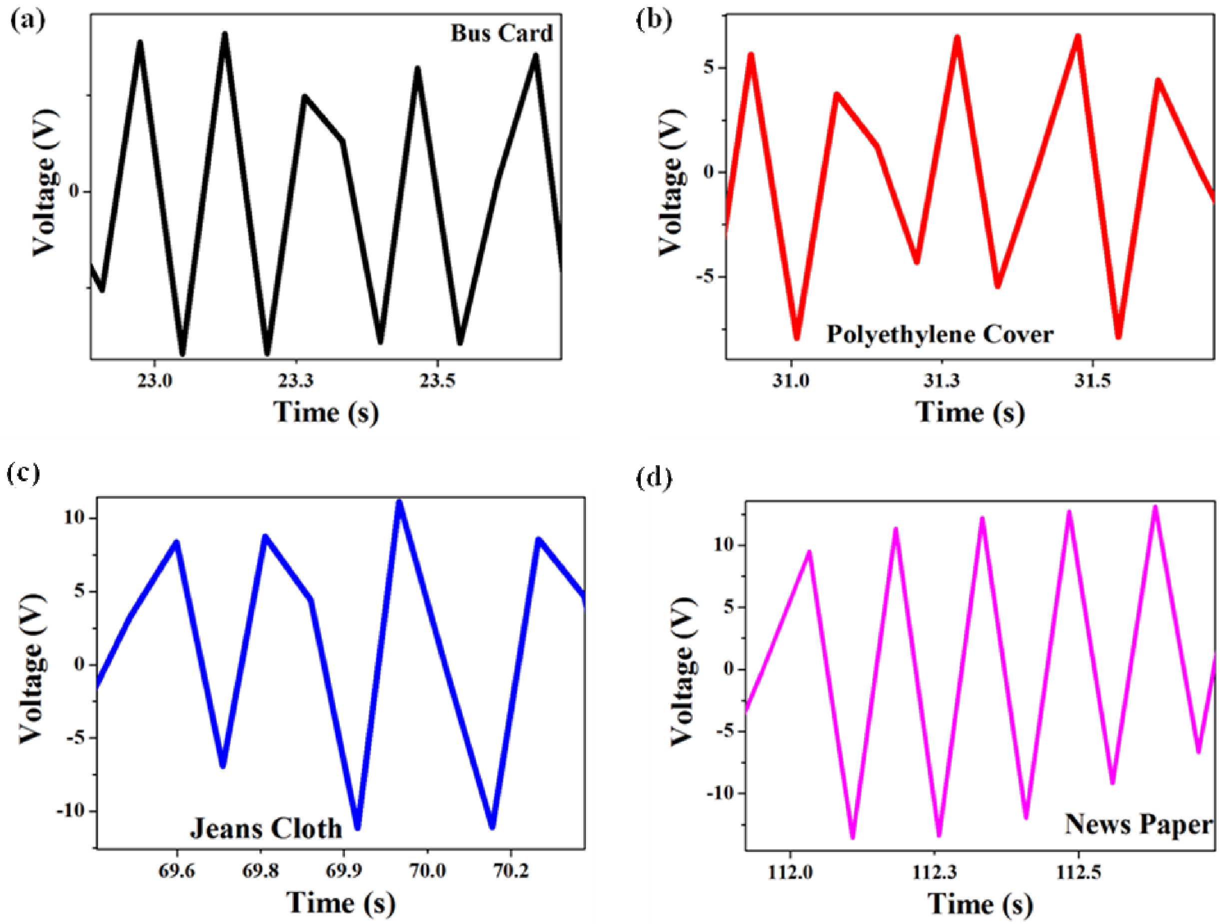


**Figure S7.** Single voltage peaks for each materials (a) Bus card, (b) Polyethylene cover, (c) Jeans and (d) News paper during contact and separation with SS-TENG device.

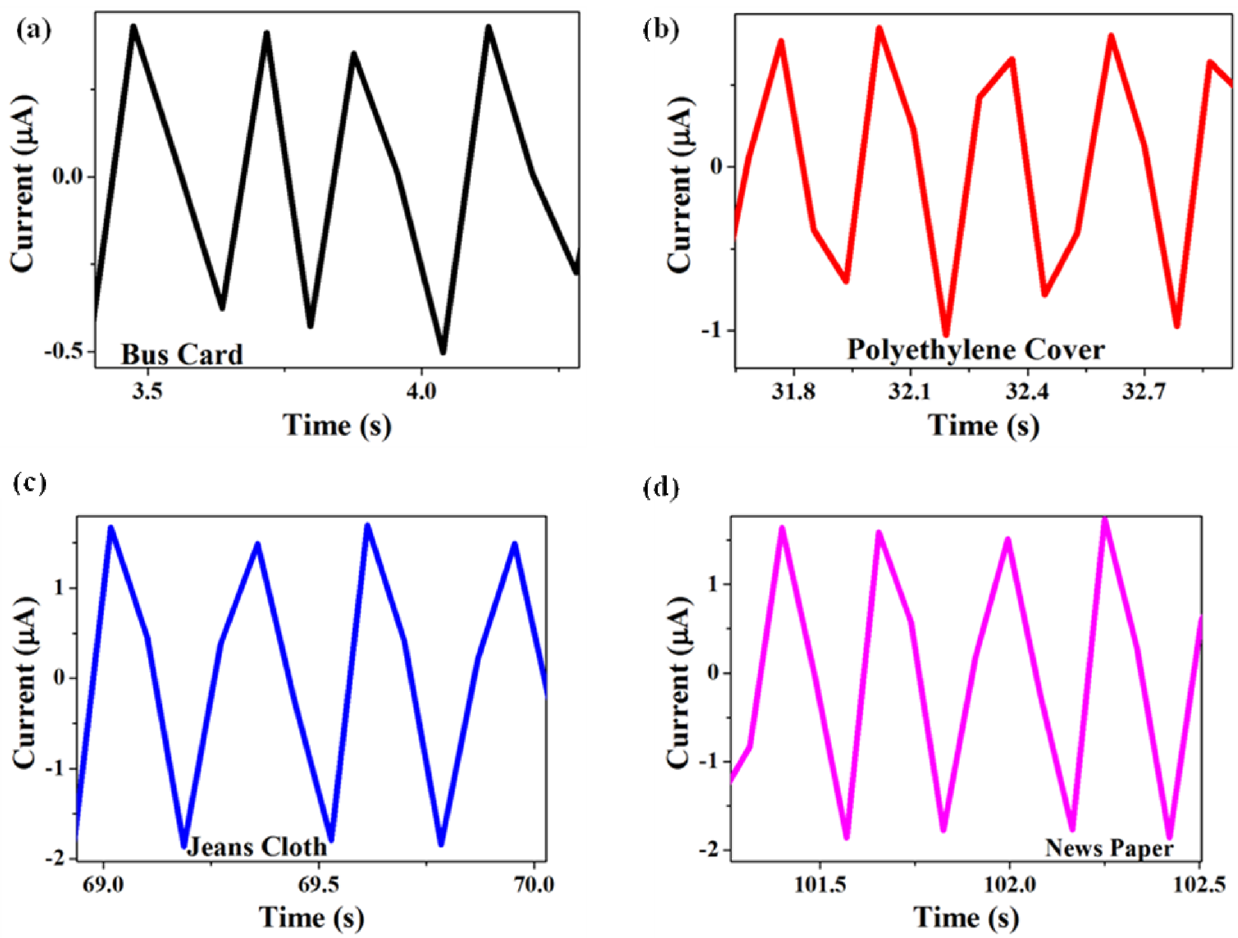


**Figure S8.** Single current peaks for each materials (a) Bus card, (b) Polyethylene cover, (c) Jeans and (d) News paper during contact and separation with SS-TENG device.

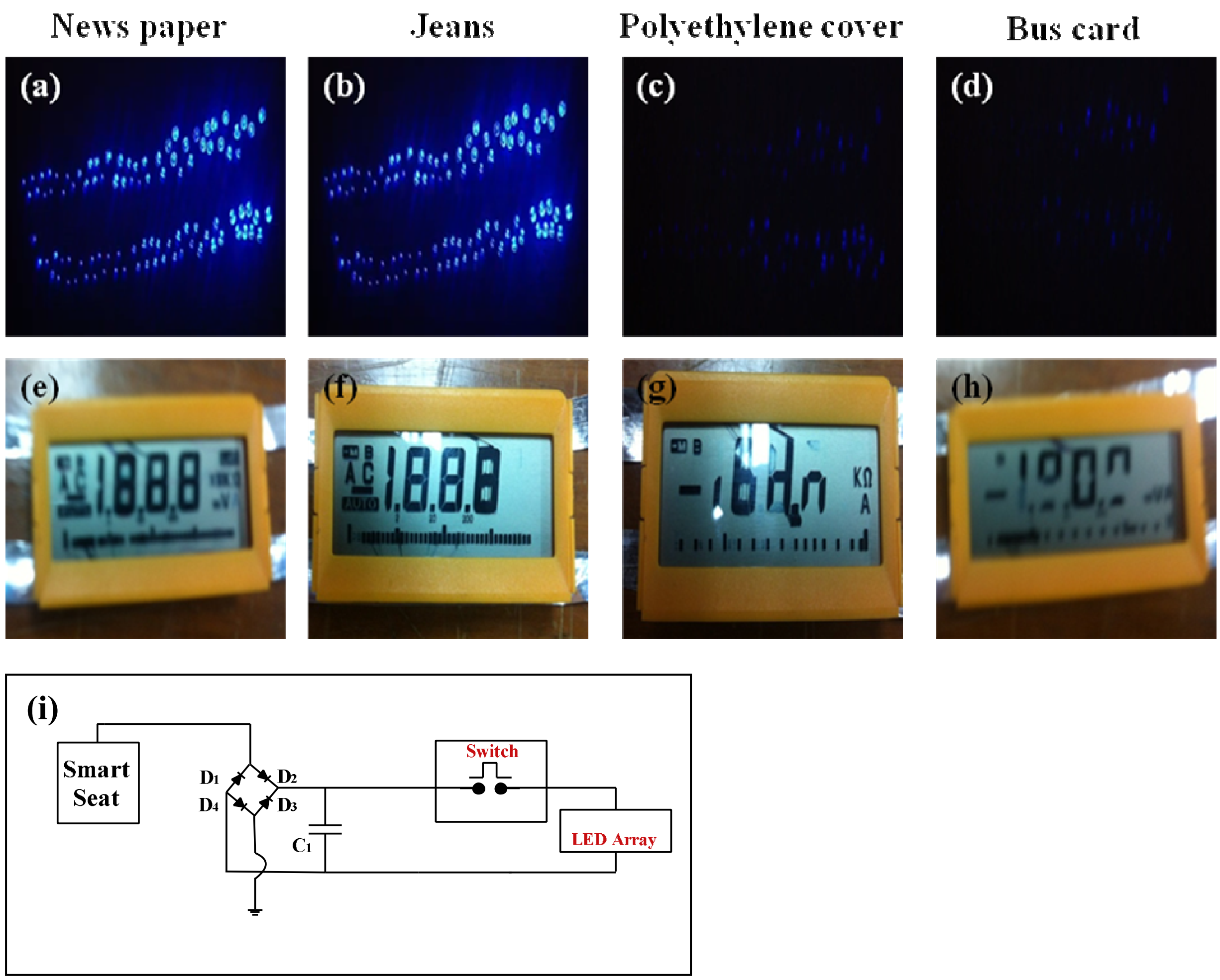


**Figure S9.** Demonstration of power management system to lit up low power electronic devices. (a-d) Photograph of 100 blue lighted LEDs in complete darkness when a single unit SS-TENG interact with different contact materials at cyclic frequency 20 Hz of Mechanical load. (e-h) Photograph of monochrome LCD display powered in ambient background lighting when a single unit SS-TENG interact with different contact materials at cyclic frequency 20 Hz of Mechanical load. (i) Complete circuit used for lighting LEDs.

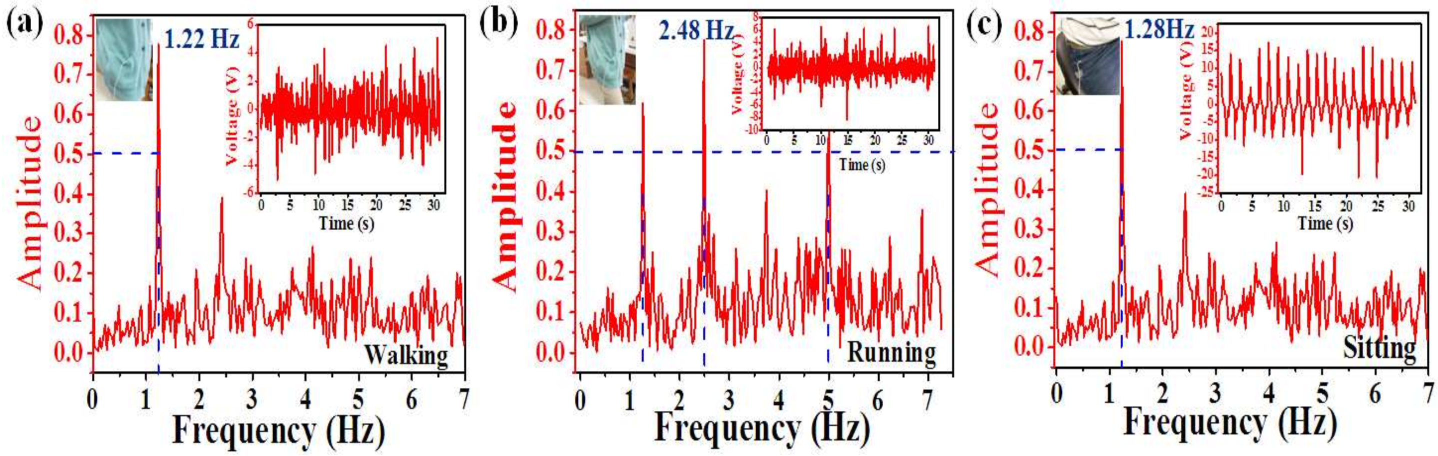


**Figure S10**. (a-c) The frequency components after Fourier transformed of the harvested voltage during human motion (walking, running, sitting).

This investigation led us to identify the frequencies of various human motions and also proved that the SS-TENG can scavenge energy from simple human motion. The Figure S10 (a-c) clearly shows the frequency of each motion (walking - 1.22 Hz, running - 2.48 Hz, sitting - 1.28 HZ) and its amplitude with respect to the generated voltage.

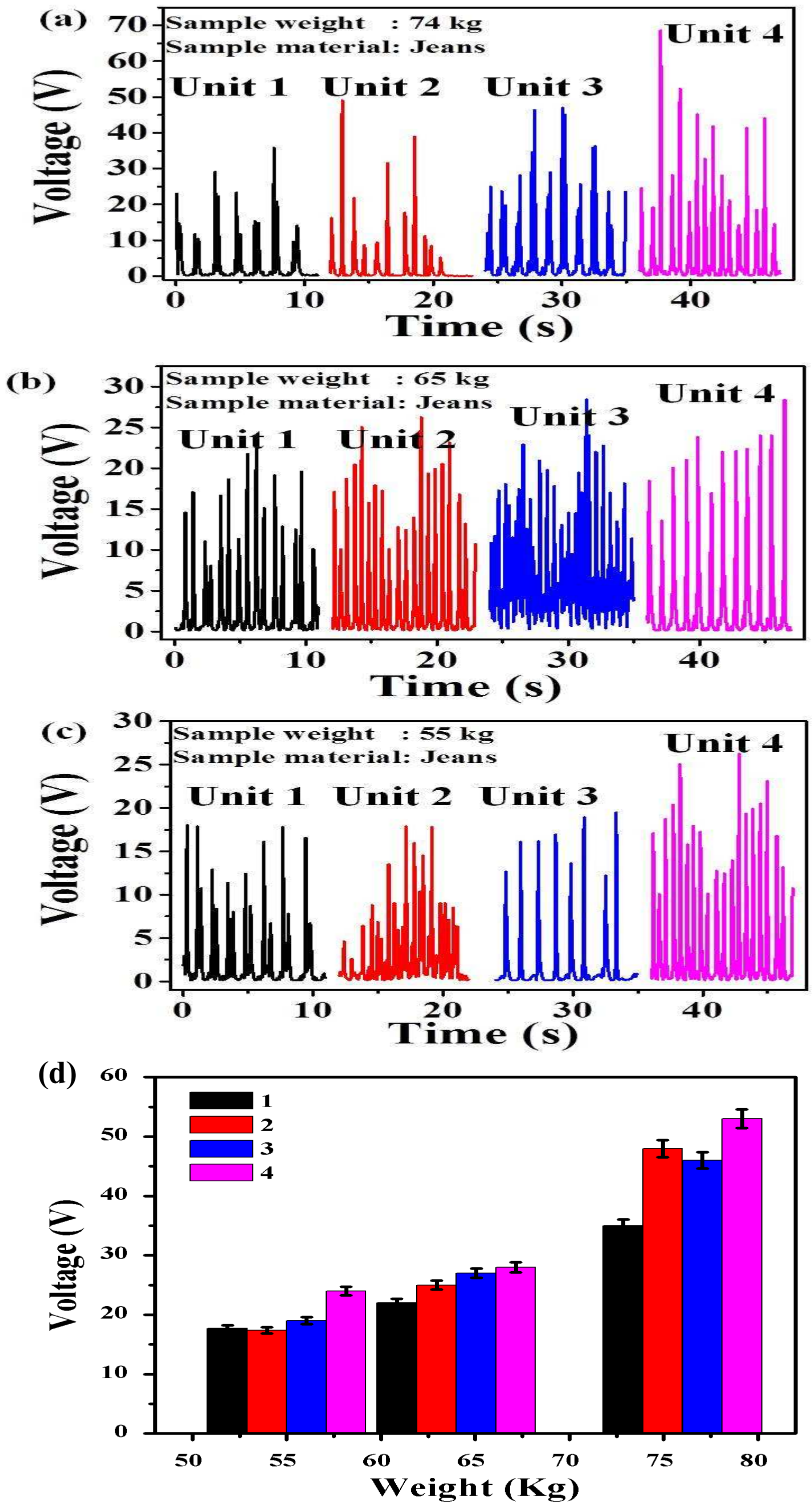


**Figure S11.** Enlarged view of the output voltage signals with different unit numbers *vs* different human weight (a-c) and error limits of real time bio-mechanical energy (d).

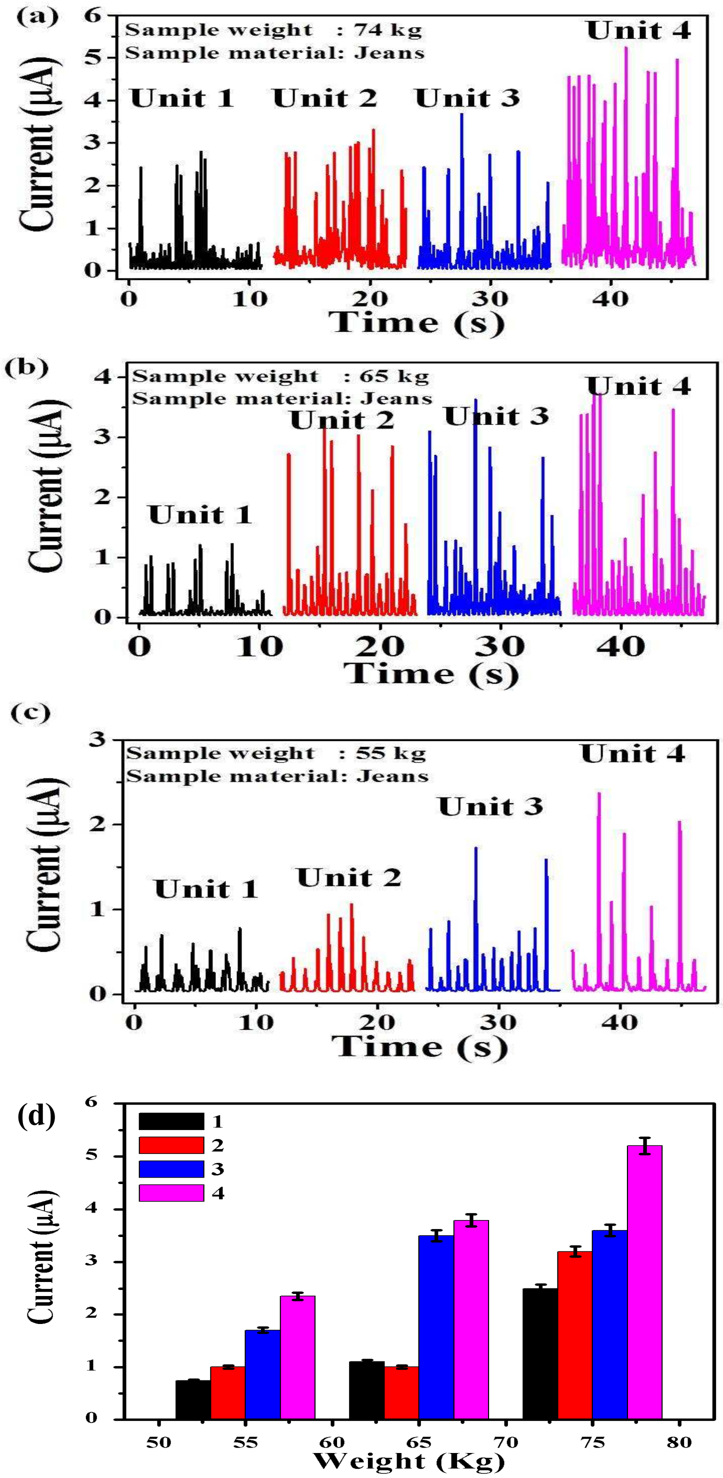


**Figure S12.** Enlarged view of the output current signals with different unit numbers *vs* different human weight (a-c) and error limits of real time bio-mechanical energy (d).

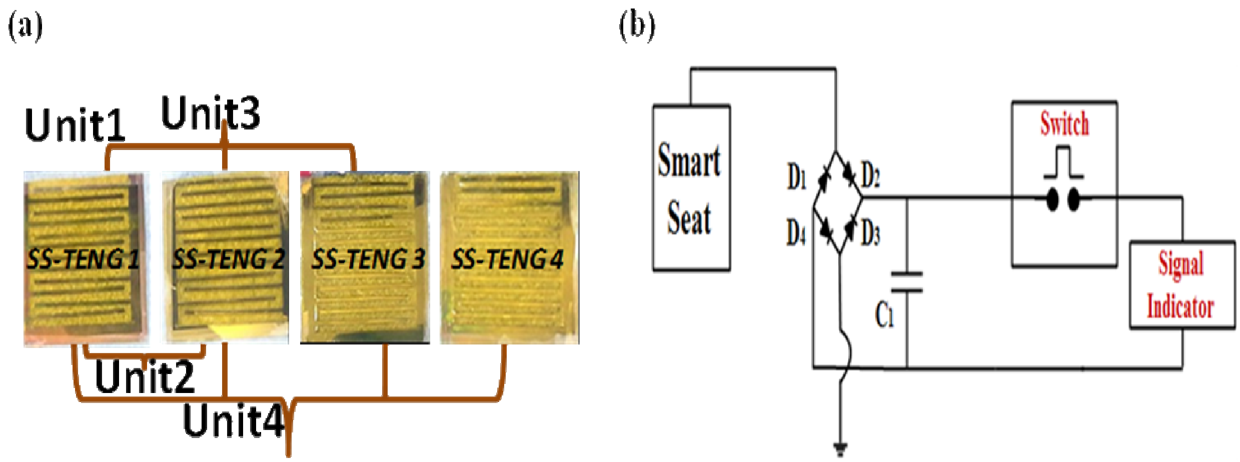


**Figure S13.** (a) Connection configuration of Multi SS-TENG. (b) Circuit connection for self-powered stop indicator lights for passenger bus.

## References


(1) Niu, S.; Wang, S.; Liu, Y.; Zhou, Y. S.; Lin, L.; Hu, Y.; Pradel, K. C.; Wang, Z. L. A Theoretical Study of Grating Structured Triboelectric Nanogenerators. *Energy Environ. Sci.* **2014**, *7*, 2339.

(2) Xie, Y.; Wang, S.; Niu, S.; Lin, L.; Jing, Q.; Yang, J.; Wu, Z.; Wang, Z. L. Grating-Structured Freestanding Triboelectric-Layer Nanogenerator for Harvesting Mechanical Energy at 85% Total Conversion Efficiency. *Adv. Mater.* **2014**, 6599–6607.

(3) Lin, Z.-H.; Cheng, G.; Li, X.; Yang, P.-K.; Wen, X.; Lin Wang, Z. A Multi-Layered Interdigitative-Electrodes-Based Triboelectric Nanogenerator for Harvesting Hydropower. *Nano Energy* **2015**, *15*, 256–265.

(4) Cope, D. K. The Edge Effect for Planar Electrodes. *J. Electroanal. Chem.* **1997**, *439*, 7–27.

(5) Gies, H.; Klingmüller, K. Casimir Edge Effects. *Phys. Rev. Lett.* **2006**, *97*, 220405.

(6) Wei, Q.; Onofrio, R. Edge Effects in Electrostatic Calibrations for the Measurement of the Casimir Force. *Phys. Lett. A* **2010**, *374*, 2230–2234.

(7) Cao, X.; Sui, X.; Lyu, Q.; Li, L.; Chai, X. Effects of Different Three-Dimensional Electrodes on Epiretinal Electrical Stimulation by Modeling Analysis. *J. Neuroeng. Rehabil.* **2015**, *12*, 73.

(8) Song, Y.; Penmatsa, V.; Wang, C. Modeling and Simulation of Enzymatic Biofuel Cells with Three-Dimensional Microelectrodes. *Energies* **2014**, *7*, 4694–4709.